

Energy Efficient Downlink mMIMO Using Dynamic Antenna and Power Adaptation

Ravi Sharan B A G*, Maliha Jada †, Anders Karstensen‡, Daniela Laselva‡, Jyri Hämäläinen§, Silvio Mandelli*

* Nokia Bell Labs, Stuttgart, Germany, Email: {ravi.bhagavathula, silvio.mandelli}@nokia-bell-labs.com

† Nokia, Finland, Email: maliha.jada@nokia.com

‡ Nokia, Denmark, Email: {anders.karstensen, daniela.laselva}@nokia.com

§ Aalto University, Finland, Email: jyri.hamalainen@aalto.fi

Abstract—Massive multiple-input multiple-output (mMIMO) technology and its future evolutions are expected to address the high data rate demands of sixth generation (6G) communication systems. At the same time, network energy savings (NES) is essential in reducing the operational costs and meeting the sustainability goals of network operators. In this regard, we propose a dynamic scheme for joint antenna and power adaptation to improve NES from a user scheduling and resource allocation perspective. Antenna adaptation is performed using the multiple channel state information resource signal (CSI-RS) framework. Furthermore, the recently introduced transmit power-aware link adaptation scheme, referred to as POLITE for short, is used as the power adaptation technique. The proposed scheme adapts to variations in users' instantaneous traffic and channel conditions to opportunistically maximize NES while also inherently accounting for the user throughput. Numerical simulation results show that the proposed scheme consistently achieves a balance between NES and user perceived throughput (UPT) for different network load conditions. Especially in low and light load conditions, the proposed scheme significantly improves the intra-cell interference and boosts the overall NES, while ensuring that UPT is unaffected.

Index Terms—6G, massive MIMO (mMIMO), Network energy savings (NES), Multiple CSI-RS framework, Link Adaptation.

I. INTRODUCTION

Standardization efforts are currently ongoing for the future fifth generation-advanced (5G-A) and sixth generation (6G) cellular wireless communication systems. These systems are envisioned to drive the advancements in emerging applications such as collaborative robots, digital twins and extended reality applications [1]. Massive multiple-input multiple-output (mMIMO) is expected to play an instrumental role in addressing the high data rate demands of both 5G-A and 6G systems [2]. This is due to the array gain and spatial multiplexing capabilities offered by large antenna arrays in mMIMO [3]. At the same time, it is becoming increasingly important for network operators to offer wireless services with reduced energy consumption and overall carbon footprint. However, maintaining a balance between network energy savings (NES) and the throughput gains can be extremely challenging. This is because next generation mMIMO gNodeBs (gNBs) are

The research work presented in this publication partially contributes to Maliha's doctoral thesis requirements at Aalto University, Finland.

expected to use even larger antenna arrays with 256 antenna ports and array sizes exceeding 1000 antenna elements [4].

Recent studies in [4]–[7] present several techniques to reduce power consumption (PC) in next generation mMIMO gNBs. Of these, antenna and power adaptation have been identified as two important NES techniques in downlink (DL). Antenna adaptation is a spatial domain technique, where gNB operates with only a subset of the available antenna ports. In this regard, [5] introduced a framework for antenna adaptation using multiple channel state information reference signal (CSI-RS) configurations. Here, each CSI-RS configuration is associated with a predefined number of antenna ports at gNB, thus enabling antenna adaptation using the CSI of associated user equipment (UE). In contrast, power adaptation is a power domain technique which focuses on the dynamic optimization of transmit power spectral density (PSD) in DL. Power optimization for low interference and throughput enhancement (POLITE) [8] is one such recent scheme, where efficient link adaptation (LA) is used to adaptively scale down PSD. Especially, POLITE efficiently utilizes the time-frequency resources to make DL transmissions robust to PSD reduction. Extending these approaches, in this work we propose a *dynamic scheme for joint antenna and power adaptation*, which aims to opportunistically improve NES while also inherently accounting for the user throughput.

In the existing literature on NES, antenna and power adaptation schemes are treated separately. The work in [9] proposed an antenna selection scheme based on the long-term temporal variations in the number of active UEs. A deep learning-based antenna selection scheme is proposed in [10] to minimize PC subject to per-UE minimum rate constraints. Here, a neural network is trained to imitate the behavior of a search-based greedy heuristic to essentially determine the set of active antennas based on the CSI of the associated UEs. In [11], the authors proposed a scheme to switch-off antenna elements for prolonged durations based on UEs' CSI. The recent work in [12] considered a PC minimization problem spanning time, space and power domains. Here, transmit power allocation is performed per each active antenna based on per-UE minimum rate requirements. However, this does not translate into PSD reduction, which involves efficient resource allocation based

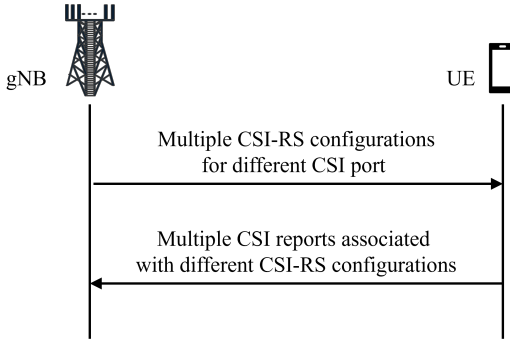


Fig. 1: Illustration of multiple CSI-RS framework

on both UE traffic and the CSI. In contrast to the prior work, in this work the interplay between LA and resource allocation aspects of antenna and power adaptation schemes is leveraged to efficiently balance the user throughput and NES.

II. NETWORK MODEL

We consider a network scenario where mMIMO gNB serves the set $\mathcal{N} := \{1, 2, \dots, N\}$, $|\mathcal{N}| = N$ of active, multi-antenna UEs in DL on same time-frequency resources. The transmission opportunity in the time-domain is represented using a slot, which is denoted by $t \in \mathbb{N}^+$. In the frequency-domain, the total available bandwidth is divided into several resource blocks (RBs) denoted by the set $\mathcal{B} := \{1, 2, \dots, B\}$, $|\mathcal{B}| = B$. We assume that gNB assigns a subset $\mathcal{B}_n \subseteq \mathcal{B}$, $|\mathcal{B}_n| = B_n$ of RBs to each UE n in an orthogonal manner. We also assume that gNB configures each UE with multiple CSI-RS configurations following [13] (see Fig. 1). Firstly, each CSI-RS configuration corresponds to gNB operating with a predefined number of CSI-RS ports, thereby facilitating antenna adaptation. Furthermore, the number of RBs required for conveying a CSI-RS configuration to a UE is directly proportional to the number of CSI-RS ports. Let $\mathcal{M} := \{1, 2, \dots, M\}$, $|\mathcal{M}| = M$ denote the set of all CSI-RS configurations. Here, each m corresponds to gNB operating with a predefined set of CSI-RS ports and transceiver chains (TRXs). Furthermore, $m = M$ corresponds to the baseline scenario, where gNB transmits in DL with all available TRXs. For other cases with $m < M, \forall m \in \mathcal{M}/\{M\}$, we assume that there is a predefined mapping to determine which CSI-RS ports and TRXs to operate at gNB.

As a consequence of UEs processing M CSI-RS configurations, gNB receives M number of channel state information (CSI) reports from each UE n . A CSI report from UE primarily comprises channel quality indicator (CQI), and additionally a rank indicator for multi-stream communication and a precoder matrix indicator. In this work, we assume that the CQI is available as a wideband metric, meaning, it is obtained at a UE by averaging the estimated signal-to-interference-plus-noise ratio (SINR) across the entire bandwidth B . Furthermore, gNB assigns a modulation and coding scheme (MCS) value to each UE n based on the corresponding received SINR estimates. Firstly, the set of MCS values that can be assigned to UEs is denoted by $\mathcal{K} = \{1, 2, \dots, K\}$, $|\mathcal{K}| = K$ w.l.o.g. Moreover,

each MCS $k \in \mathcal{K}$ is associated with a transmission rate $R(k)$. The link reliability of each UE n is evaluated using the achievable block error rate (BLER), which is denoted by $\epsilon_n(\gamma_{n,m}; k)$. Moreover, the desired target BLER for the first transmission attempt is denoted by $\bar{\epsilon}$. Furthermore, the SINR estimate at a UE n and associated with the m^{th} CSI configuration is denoted as $\gamma_{n,m} := S_{n,m} \cdot \hat{\alpha}_{n,m}$. Here, $\hat{\alpha}_{n,m} \in \mathbb{R}$ collectively represents the channel and noise-plus-interference estimate of a UE n associated with the m^{th} CSI report. The term $S_{n,m}$ represents the PSD of a UE n with respect to the m^{th} CSI-RS configuration and is given by:

$$S_{n,m} = \frac{P_{n,m}}{B_n}, \quad (1)$$

where, $P_{n,m} \leq \bar{P}_m$ is the power allocated to UE n when m^{th} CSI-RS configuration is used. The term \bar{P}_m is the maximum allowable transmit power associated with the m^{th} CSI-RS configuration. Finally, the number of bits pending for transmission at n^{th} UE's buffer is denoted by $Q_n \leq \bar{Q}$, with \bar{Q} being the maximum number of bits allowed in the buffer. Based on the notation presented here, an overview of medium access control (MAC) operations are provided in the next section.

III. MAC LAYER OPERATIONS

In this section, we first discuss the resource scheduling aspects of the MAC scheduler. This is followed by an overview of LA schemes explained from the perspective of antenna adaptation and the POLITE scheme. Firstly, given the set of active UEs \mathcal{N} , the task of the MAC layer is to select appropriate MCS and allocate per-slot resources or RBs among these UEs. In practice, resource scheduling is performed using the widely adopted proportional fair (PF) scheduler due to its strong performance guarantees in MIMO systems [8], [14]. More specifically, the PF scheduler allocates RBs to UEs based on a per-UE metric obtained on each RB b as follows:

$$X_n(b) = \frac{R_n(k; b)}{R_{n,\text{avg}}}, \quad \forall b \in \mathcal{B}. \quad (2)$$

Here, $R_n(k; b)$ is the MCS-dependent instantaneous rate of UE n on the b^{th} RB and $R_{n,\text{avg}}$ is the running average of n^{th} UE's throughput. In essence, the PF metric allocates a RB to a UE with high spectral efficiency relative to its recent throughput history. Doing so, the PF metric ensures that RBs are proportionately allocated to UEs on an average in time.

As a consequence of considering the wideband CQI in this work, Equation (2) reduces to a *single metric* per-UE across the entire bandwidth B . This also facilitates the use of greedy approaches to solve the originally NP-hard RB allocation problem. One such approach involves allocating contiguous subset of RBs to UEs simply based on the estimated number of RBs, which can be obtained as a function of the MCS value [14]. Since LA is essentially responsible for determining the MCS values of UEs, the remainder of this section focuses on the LA schemes considered in this work.

The LA is performed for every UE $n \in \mathcal{N}$ to determine the optimal MCS by solving a rate maximization problem with

BLER requirements incorporated as constraints. Especially when each UE $n \in \mathcal{N}$ is configured with M CSI-RS configurations, LA is also performed for all M configurations [15]. In this case, the LA problem at UE $n \in \mathcal{N}$ for the m^{th} CSI-RS configuration can be written as follows:

$$\mathbf{P1:} \underset{k}{\text{maximize}} \quad R_n(k) \quad (3a)$$

$$\text{subject to } \epsilon_n(\gamma_{n,m}; k) \leq \bar{\epsilon} \quad (3b)$$

$$S_{n,m} \leq \bar{S}_{n,m}, \quad k \in \mathcal{K}, \quad \forall m \in \mathcal{M}. \quad (3c)$$

Here, the term $\bar{S}_{n,m}$ is the maximum allowable PSD derived with respect to \bar{P}_m . Thus, the change in maximum allowable transmit power due to operating with multiple CSI-RS configurations is reflected through the right hand side of the constraint (3c). Moreover, it can be observed that **P1** is a straightforward extension of baseline LA with $m = M$ to the network setup with multiple CSI-RS configurations. As a consequence of this, the solution approach of the baseline LA can also be extended to any $m < M$, where the MCS k is greedily determined in the reference configuration using an upper bound on constraints (3b) and (3c).

A. Overview of POLITE

The original concept of POLITE [8] is essentially aimed at minimizing PSD of DL transmissions by refining UEs' MCS values determined using the baseline LA with $m = M$. More specifically, POLITE uses the buffer information of UEs available at MAC layer to effectively reduce the MCS values of UEs while still satisfying the target BLER requirements. Consequently, this leads to an increase in the number of RBs allocated to UEs, thereby enabling DL transmissions with an overall lower PSD compared to the baseline LA. Formally, POLITE concept can be expressed in terms of LA using the following optimization problem:

$$\mathbf{P2:} \underset{k'}{\text{minimize}} \quad S_{n,m}(k') \quad (4a)$$

$$\text{subject to } R_n(k') \geq \beta_n \cdot R_n(k) \quad (4b)$$

$$\epsilon_n(\gamma_{n,m}; k') \leq \bar{\epsilon} \quad (4c)$$

$$k' \leq k, \quad \forall k, k' \in \mathcal{K}, \quad \forall n \in \mathcal{N}. \quad (4d)$$

Firstly, it can be observed that PSD $S_{n,m}$ is now a function of the MCS value k' . This dependency on MCS is reflected in (1) through the denominator, rendering B_n as a function of MCS k (or k' in (4)). Secondly, the objective and the constraints are reversed in **P2** when compared to baseline LA. Especially, the inclusion of constraint (4b) ensures that the achievable rate is not affected as a consequence of operating with a lower MCS due to POLITE. Finally, the BLER constraint in (4c) is the same as the baseline LA.

The solution approach of POLITE revolves around modeling the linear rate-adaptation parameter β_n in the constraint (4b). While there are several ways of evaluating the β_n term [16], in this work we resort to using the load-driven POLITE variant [8]. More specifically, the β_n value is derived as a function of the buffer value Q_n of a UE n and the total bandwidth B at current slot as in [8]. Accordingly, this

provides a way to balance PSD reduction without compromising on the achievable throughput. Formally, β_n value of UE n following the load-driven approach can be expressed as follows:

$$\beta_n := \min \left[\chi \cdot \sum_{n \in \mathcal{N}} \frac{Q_n}{R_{n,\text{avg}} \cdot B}, 1 \right], \quad (5)$$

where, $\chi \in (0, 1]$ is a predefined multiplicative factor used to avoid abrupt changes in β_n and $R_{n,\text{avg}}$ is the time-averaged throughput of UE n as described above. Firstly, evaluating per-UE β_n in this manner is termed load-driven POLITE, since the users' packet arrivals influence the RB usage or the network load of the current slot t . Another noticeable aspect of (5) is that despite indexing with respect to each UE n , β_n is derived as a joint metric across all the associated UEs in the network.

IV. DYNAMIC ANTENNA AND POWER ADAPTATION

In this work, a dynamic scheme for joint antenna and power adaptation is proposed, which opportunistically maximizes NES at gNB while inherently accounting for user throughput. More specifically, both antenna adaptation and power adaptation decisions are optimized together on a per-slot basis by leveraging the LA schemes discussed in the previous section. In this regard, antenna adaptation is performed first as it results in a higher reduction in gNB PC [4]. More specifically, number of active TRXs are determined by solving the LA problem in (3). This is followed by performing POLITE-based power adaptation as described in (4). The motivation behind using POLITE after antenna adaptation is to efficiently counter the intra-cell interference. More specifically, as gNB operates with fewer TRXs, the beams used for DL transmissions to UEs become wider, thereby causing interference in the frequency-domain. However, as POLITE is more likely to reduce the MCS of UEs with higher MCS, it effectively leads to DL transmissions with reduced transmit power and eventually less interference. Thus, sequentially performing antenna adaptation and POLITE through efficient LA and RB allocation leads to maximizing NES, while delivering throughput to UEs. A detailed overview of the steps involved in the proposed scheme are presented in **Alg. 1**.

In **Alg. 1**, step 1 is evaluated using Equation (2) based on MCS obtained using the reference configuration with $m = M$. Furthermore, steps 2 — 10 correspond to antenna adaptation, where the number of active antenna ports for DL transmissions in the current slot are determined in a greedy manner. Here, \mathcal{M}^* in step 2 refers to the set \mathcal{M} arranged in the reverse order. More importantly, antenna adaptation is performed if and only if the corresponding RB allocation allows for emptying the buffers of all the associated UEs. Steps 13 and 14 correspond to POLITE LA as described in Section III-A, where $m = m'$ is substituted instead of $m = M$ as in (4). In steps 15—19, any remaining RBs are distributed among UEs whose buffers still have pending bits. It can be seen from **Alg. 1** that antenna and power adaptation decisions effectively take into account the CSI and buffer information of UEs at each slot. Secondly, **Alg. 1** essentially works by leveraging the PSD

expression in (1). More specifically, the steps corresponding to antenna adaptation result in reduced transmit power $P_{n,m}$ in (1). Finally, the steps associated with POLITE LA and the remaining steps result in an overall reduction of $S_{n,m}$ due to a decrease in UEs' MCS values and an increase in the allocated RBs.

Algorithm 1 Dynamic Antenna and Power Adaptation Scheme

Initialize: $m \leftarrow M, m' \leftarrow m, \tilde{k}_n \leftarrow 0, \forall n \in \mathcal{N}$.
Input: $k_n, \forall n \in \mathcal{N}$ using reference configuration $m = M$.

- 1: Arrange UEs in the descending order of $\{X_n\}_{n=1}^N$ (2).
- 2: **for each** $m \in \mathcal{M}^*/\{M\}$ **do**
- 3: $\tilde{k}_n \leftarrow k_n, \forall n \in \mathcal{N}$.
- 4: Obtain k_n and B_n by solving (3), $\forall n \in \mathcal{N}$.
- 5: **if** $Q_n, \forall n \in \mathcal{N}$ can be emptied **then**
- 6: $m' \leftarrow m$.
- 7: **else**
- 8: $m' \leftarrow m + 1$.
- 9: $k_n \leftarrow \tilde{k}_n, \forall n \in \mathcal{N}$.
- 10: **go to** Step 13.
- 11: **end if**
- 12: **end for**
- 13: Compute $\beta_n, \forall n \in \mathcal{N}$ following (5).
- 14: Update k_n and B_n by solving (4), $\forall n \in \mathcal{N}$.
- 15: **if** $B - \sum_{n \in \mathcal{N}} B_n > 0$ **then**
- 16: Recompute $\{X_n\}_{n=1}^N$ using (2).
- 17: Arrange UEs in the descending order of $\{X_n\}_{n=1}^N$.
- 18: Allocate remaining RBs among UEs with $Q_n > 0$.
- 19: **end if**
- 20: **return** $m', k_n, B_n, \forall n \in \mathcal{N}$.

V. NUMERICAL SIMULATIONS

In this section, we present the performance evaluations of **Alg. 1** using numerical simulation results. To this extent we use a third generation partnership project (3GPP) compliant system level simulator modeled using the design principles presented in [17]. However, prior to presenting the numerical results, we first briefly discuss the key performance indicators (KPIs) and the simulation methodology used for the performance evaluation.

A. Simulation Methodology

In this work, we use two KPIs to evaluate the performance of the algorithms considered for numerical simulation results. The first KPI corresponds to user perceived throughput (UPT), which is defined as the average application layer throughput per File Transfer Protocol 3 (FTP3) packet transmission. Here, the averaging is performed both with respect to the number of transmitted packets of all UEs and the total simulation duration. The second KPI corresponds to NES expressed in terms of gNB PC, which is evaluated using the 3GPP PC model [5] as described below.

The 3GPP PC model is characterized by different sleep states, namely the micro, light and deep sleep states. Firstly,

no transmission or reception takes place when gNB operates in a sleep state. Secondly, each sleep state corresponds to the case where one or more hardware components of gNB are switched off, with majority of components being switched off in the deep sleep state. Furthermore, the PC associated with each sleep state is expressed in relative units in reference to the deep sleep state PC. The use of relative units instead of absolute units (e.g. Watts) provides an efficient abstraction of gNB implementations from different telecommunication network equipment vendors.

The 3GPP PC model also defines active state PC values resulting from dynamic operations of gNB in each slot. An active state here refers to the time period during which data transmission takes place in DL and/or uplink directions. As this work pertains to DL transmissions, only the relevant DL PC expressions are provided here. The DL PC in the active state due to per-slot gNB operations are expressed as a combination of static and dynamic terms, which can be formally expressed as follows:

$$PC_{\text{active}} = s_a \left(s_f \cdot s_p \cdot \frac{P_{\text{dyn, joint}}}{\eta(s_f, s_p)} + P_{\text{dyn, ante}} \right) + P_{\text{static}}. \quad (6)$$

The parameters s_a , s_f and s_p denote the ratio of active TRXs to the total TRXs, the ratio of occupied bandwidth to the system bandwidth, and the ratio of PSD between the DL transmission and reference configuration from [18, Table II]. Furthermore, $\frac{P_{\text{dyn, joint}}}{\eta(s_f, s_p)}$ is the PC associated with the power amplifier, which is a function of the transmit power, number of TRXs and the operating bandwidth. The term η is the power amplifier efficiency parameter, which is modeled as a function of s_f and s_p factors as described in [18]. Furthermore, $P_{\text{dyn, ante}}$ corresponds to PC associated with hardware components such as digital front-end, which scales only as function of the active TRXs. Finally, P_{static} corresponds to PC of essential hardware components which are required to keep gNB operational in active and sleep states.

The results are generated for four different traffic or network load conditions, namely low, light, medium and high loads as specified in [5]. The load conditions are modeled as a function of packet arrivals at UEs, where packets are generated using the FTP3 traffic model. Furthermore, we consider five baseline schemes in this work. Of these, three baselines correspond to static antenna configurations with 8, 16 and 32 maximum number of gNB TRXs, which are referred to as **Static8**, **Static16** and **Static32**, respectively. In addition to these baselines, we also consider a dynamic antenna adaptation and a power adaptation scheme as baselines in this work. In the antenna adaptation scheme, referred to as **Antenna Adaptation** in the results, the number of active TRXs are dynamically determined from the set {32, 16, 8}. Furthermore, POLITE is used as the power adaptation baseline and is referred to as **Power Adaptation** in the numerical results. Finally, the parameters used for generating the numerical results are summarized in Table I.

Parameter	Value
Number of gNBs	21
Total number of UEs	210
Maximum number of gNB TRXs	32
UE configuration	Single antenna UEs
Channel model	38.901 UMa NLoS [19]
MIMO mode	Single User MIMO
Duplexing protocol	TDD
Bandwidth	100 MHz
OFDM subcarrier spacing	30 kHz
Carrier frequency	3.5 GHz
Maximum transmit power at gNB	52 dBm
Precoder type	Type-I
MCS table	Table 5.1.3.1-2 [13]
Packet arrival rate at UEs	{100, 180, 340, 500}
Packet size	5 Kbytes
Maximum HARQ retransmissions	4
Number of simulation drops	10
Number of slots per drop	28000

TABLE I: Numerical Simulation Parameters

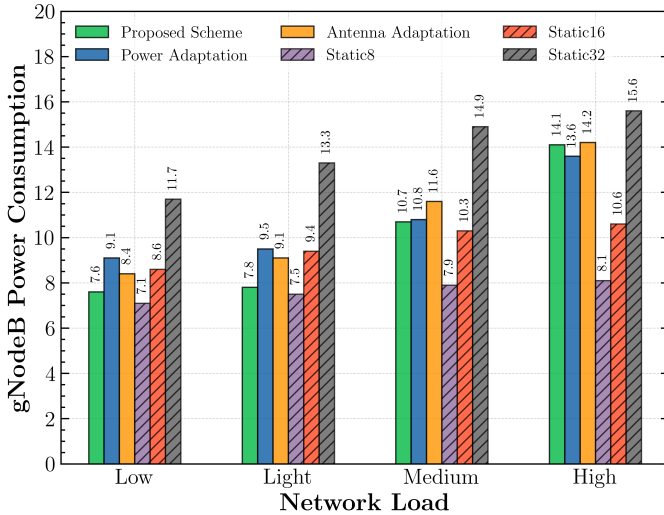


Fig. 2: Comparison of power consumption vs network load

B. Results Discussion

We begin the performance evaluation by comparing gNB PC and UPT performance in Figs. 2 and 3, respectively. Firstly, the proposed scheme *consistently* results in a lower PC compared to Static32 in all load conditions. More importantly, NES here is achieved without any significant degradation in UPT. Secondly, PC of the proposed scheme is on par with Static8 in low and light load conditions. In medium and high load conditions, Static8 and Static16 comparably result in a lower PC. However, both these baselines fair poorly in terms of UPT compared to the proposed scheme. This establishes the need for a dynamic NES scheme that can adapt to traffic and CSI of UEs as proposed in this work.

Furthermore, PC of the proposed scheme is less than that of Antenna Adaptation and Power Adaptation in low and light load conditions and it is comparable with both these schemes in medium and high load conditions. That said, UPT of the proposed scheme is consistently on par with both these schemes in all load conditions. This shows the importance

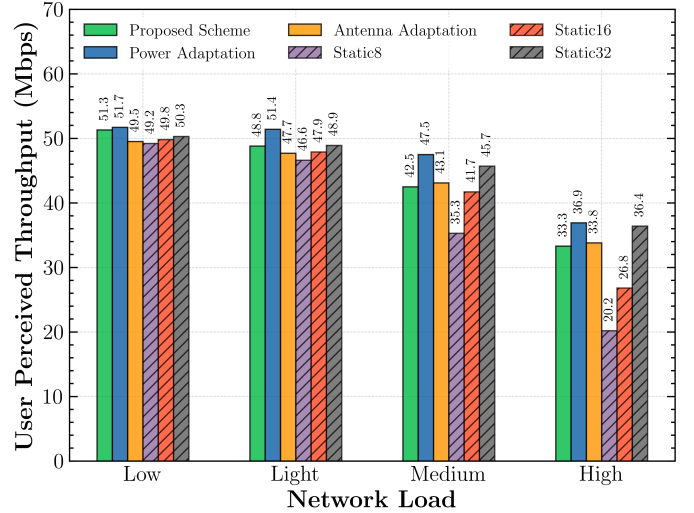


Fig. 3: Comparison of user throughput vs network load

of jointly optimizing antenna and power adaptation schemes through efficient resource allocation, as described in **Alg. 1**. Overall, the proposed scheme strikes a good balance between NES and UPT under varying traffic and channel conditions.

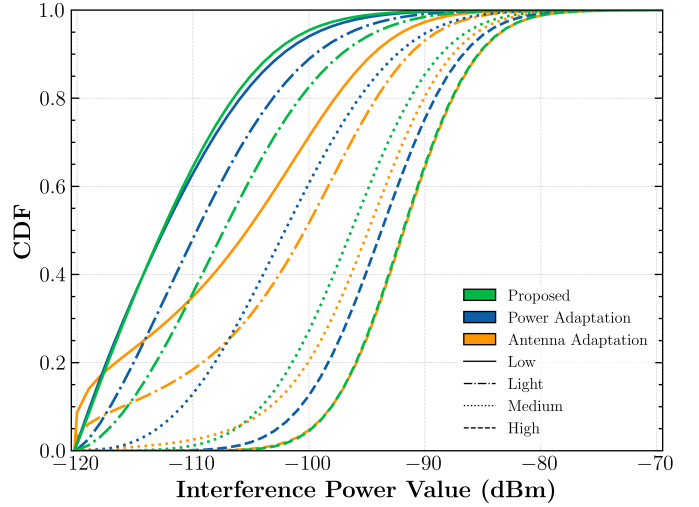


Fig. 4: Empirical distribution of interference power values

In Fig. 4, the empirical distribution of intra-cell interference power value (IPV) is plotted, where IPV is sampled per RB. Firstly, the proposed scheme induces very low intra-cell interference in low and light load conditions. While IPV increases with the load, it is still induces less interference or is comparable with IPV distribution of Antenna Adaptation. This can be attributed to the interplay between LA and resource allocation in the proposed scheme in **Alg. 1**. Finally, in Fig. 5, we compare the RB utilization of the proposed scheme with the baselines. It can be seen that the proposed scheme consistently results in high RB usage. Secondly, the RB usage of the proposed scheme is almost comparable with that of the POLITE-based power adaptation. This, together with NES and

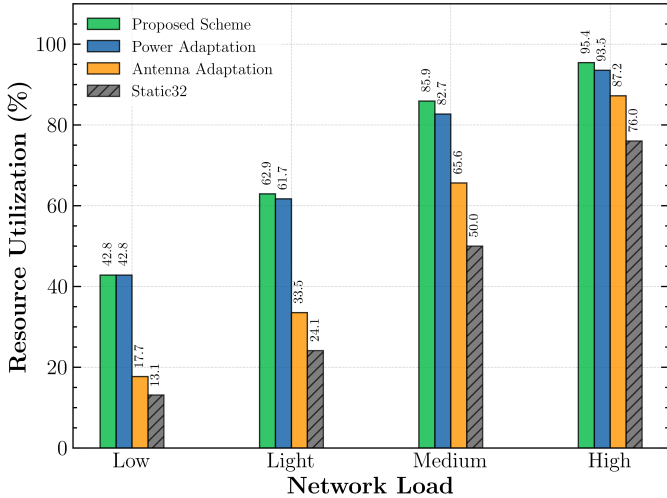


Fig. 5: Comparison of resource utilization vs network load

UPT performance in Figs. 2 and 3 shows that efficient resource allocation plays a key role in balancing UPT and NES.

VI. CONCLUSIONS

In this work, a dynamic scheme for joint antenna and power adaptation scheme is proposed at the MAC scheduler to efficiently balance between NES and UPT in DL at a mMIMO gNB. More specifically, the proposed scheme efficiently adapts to both CSI and traffic conditions of the associated UEs, which can be extremely beneficial in power-hungry mMIMO deployments. Numerical simulation results generated using a 3GPP compliant simulator demonstrate that the proposed scheme achieves the intended balance between NES and UPT for all traffic load conditions. Especially in low and light load conditions, the proposed scheme achieves NES gains of $\approx 35\% - 41\%$ compared to static antenna adaptation baselines. This is noteworthy since antenna adaptation and POLITE-based power adaptation are performed in a sequential manner by efficiently leveraging LA and resource allocation. Future work will focus on solutions to overcome the CSI acquisition limitations of the multiple CSI-RS framework to further improve NES and UPT in 6G mMIMO-based gNBs.

REFERENCES

- [1] M. A. Uusitalo, H. Farhadi, M. Boldi, M. Ericson, G. Fettweis, B. M. Khorsandi, I. L. Pavón, M. Mueck, A. Nimr, A. Pärssinen, B. Richerzhagen, P. Rugeland, D. Sabella, and H. Wymeersch, "Toward 6G — Hexa-X Project's Key Findings," *IEEE Communications Magazine*, vol. 63, no. 5, pp. 142–148, 2025.
- [2] Z. Wang, J. Zhang, H. Du, D. Niyato, S. Cui, B. Ai, M. Debbah, K. B. Letaief, and H. V. Poor, "A tutorial on extremely large-scale mimo for 6g: Fundamentals, signal processing, and applications," *IEEE Communications Surveys & Tutorials*, vol. 26, no. 3, pp. 1560–1605, 2024.
- [3] E. Björnson, J. Hoydis, L. Sanguinetti *et al.*, "Massive MIMO networks: Spectral, energy, and hardware efficiency," *Foundations and Trends® in Signal Processing*, vol. 11, no. 3-4, pp. 154–655, 2017.
- [4] S. Wesemann, J. Du, and H. Viswanathan, "Energy Efficient Extreme MIMO: Design Goals and Directions," *IEEE Communications Magazine*, vol. 61, no. 10, pp. 132–138, 2023.
- [5] 3GPP, "Study on Network Energy Savings for NR (Release 18)," 3rd Generation Partnership Project (3GPP), Technical Report 38.864, 2023.
- [6] D. López-Pérez, A. De Domenico, N. Piovesan, G. Xinli, H. Bao, S. Qitao, and M. Debbah, "A Survey on 5G Radio Access Network Energy Efficiency: Massive MIMO, Lean Carrier Design, Sleep Modes, and Machine Learning," *IEEE Communications Surveys & Tutorials*, vol. 24, no. 1, pp. 653–697, 2022.
- [7] D. Laselva *et al.*, "White paper: The Path to 6G with Unparalleled Energy Savings – A 3GPP Standardization Perspective," Nokia, Tech. Rep., 2024.
- [8] S. Mandelli, A. Lieto, P. Baracca, A. Weber, and T. Wild, "Power Optimization for Low Interference and Throughput Enhancement for 5G and 6G systems," in *2021 IEEE Wireless Communications and Networking Conference Workshops (WCNCW)*, 2021, pp. 1–7.
- [9] M. M. A. Hossain, C. Cavdar, E. Björnson, and R. Jäntti, "Energy Saving Game for Massive MIMO: Coping With Daily Load Variation," *IEEE Transactions on Vehicular Technology*, vol. 67, no. 3, pp. 2301–2313, 2018.
- [10] N. Rajapaksha, J. Mohammadi, S. Wesemann, T. Wild, and N. Rajatheva, "Minimizing Energy Consumption in MU-MIMO via Antenna Muting by Neural Networks With Asymmetric Loss," *IEEE Transactions on Vehicular Technology*, vol. 73, no. 5, pp. 6600–6613, 2024.
- [11] W. Pramudito, E. Alsusa, A. Al-Dweik, K. A. Hamdi, D. K. C. So, and T. L. Marzetta, "Load-Aware Energy Efficient Adaptive Large Scale Antenna System," *IEEE Access*, vol. 8, pp. 82 592–82 606, 2020.
- [12] E. Peschiera, Y. Agram, F. Quitin, L. V. der Perre, and F. Rottenberg, "On Optimizing Time-, Space- and Power-Domain Energy-Saving Techniques for Sub-6 GHz Base Stations," 2025. [Online]. Available: <https://arxiv.org/abs/2505.15445>
- [13] 3GPP, "NR; Physical layer procedures for data," 3rd Generation Partnership Project (3GPP), Technical Specification (TS) 38.214, 07 2025, version 18.7.0. [Online]. Available: <https://portal.3gpp.org/desktopmodules/Specifications/SpecificationDetails.aspx?specificationId=3216>
- [14] S.-B. Lee, S. Choudhury, A. Khoshnevis, S. Xu, and S. Lu, "Downlink MIMO with Frequency-Domain Packet Scheduling for 3GPP LTE," in *IEEE INFOCOM 2009*, 2009, pp. 1269–1277.
- [15] 3GPP, "NR; Physical layer procedures for data," 3rd Generation Partnership Project (3GPP), Technical Specification (TS) 38.300, 10 2025, version 18.7.0. [Online]. Available: <https://portal.3gpp.org/desktopmodules/Specifications/SpecificationDetails.aspx?specificationId=3216>
- [16] S. Mandelli, A. Lieto, M. Razenberg, A. Weber, and T. Wild, "Reducing interference via link adaptation in delay-critical wireless networks," *EURASIP Journal on Wireless Communications and Networking*, vol. 2022, no. 1, p. 109, 2022.
- [17] K. I. Pedersen, R. Maldonado, G. Pocovi, E. Juan, M. Lauridsen, I. Z. Kovács, M. Brix, and J. Wigard, "A Tutorial on Radio System-Level Simulations With Emphasis on 3GPP 5G-Advanced and Beyond," *IEEE Communications Surveys & Tutorials*, vol. 26, no. 4, pp. 2290–2325, 2024.
- [18] D. Laselva, S. Hakimi, M. Lauridsen, B. Khan, D. Kumar, and P. Mogensen, "On the Potential of Radio Adaptations for 6G Network Energy Saving," in *2024 Joint European Conference on Networks and Communications & 6G Summit (EuCNC/6G Summit)*, 2024, pp. 1157–1162.
- [19] 3GPP, "Study on channel model for frequencies from 0.5 to 100 GHz," 3rd Generation Partnership Project (3GPP), Technical Specification (TS) 38.901, 05 2024, version 18.0.0. [Online]. Available: <https://portal.3gpp.org/desktopmodules/Specifications/SpecificationDetails.aspx?specificationId=3173>